Charge-carrier statistics at InAs/GaAs quantum dots

O. Engström[1,*] and P. T. Landsberg[2]
[1]*Department of Microtechnology and Nanoscience, Chalmers University of Technology, SE-412 96 Göteborg, Sweden*
[2]*Faculty of Mathematical Studies, University of Southampton, Southampton S09 5NH, United Kingdom*
(Received 9 November 2004; revised manuscript received 10 May 2005; published 26 August 2005)

The statistics of thermal electron emission from InAs/GaAs quantum dots with base/height dimensions of 20/10 (nm) are developed. The quantum dots considered are assumed to have two electron energy levels. For the electrons captured in the ground state, this gives the possibility of two different emission paths. Starting from a grand canonical ensemble and using an idea for "truncated cascade capture," we derive "effective thermal emission rates" corresponding to experimental quantities. From experimental data of the capture cross sections, we demonstrate that the thermal emission path for electrons is shifted when the temperature is changed. In an Arrhenius plot for electron emission rates from the ground state, this is manifested as a transition region with varying slope which does not give any information about activation energies. The position on a temperature scale of this transition region depends on the internal relaxation time for electrons to go from the excited to the ground states. Due to limitations of experimental setups normally used for measuring activation energies, such measurements are done within a very limited temperature range. Erroneous interpretations of measured data therefore may occur if the possibility of a change in emission path is not taken into account. A method to avoid this problem in an experimental situation is pointed out in the discussion.

DOI: 10.1103/PhysRevB.72.075360   PACS number(s): 73.21.La, 73.22.Dj

I. INTRODUCTION

For quantum dots (QDs) embedded in a semiconductor matrix, the emission and capture of charge carriers have a resemblance with the corresponding phenomena of recombination centers.[1–5] Their electron potentials confine the charge carriers to orbitals similar to those in impurity atoms.[6–8] The most extensively investigated system, the InAs/GaAs combination, has InAs dots with base/height dimensions of about 20/10 (nm) embedded in a GaAs matrix and gives rise to discrete energy levels with only a few electrons captured. For the InAs/GaAs system, theory and experiments have demonstrated that in most cases two different electron shells exist inside the dots. The eigen energies of their electron states are dependent on dot dimension, shape, orientation, and chemical composition. In general, for 20/10 (nm) dots, discussed in the present work, an electron shell with s character is found at an energy level of about 150 meV from the GaAs conduction band, and a p shell occurs about 50 meV above the s ground states. The s shell can accept two electrons with opposite spins. Due to the flattened shape of the dots, one of the p orbitals receives an eigen energy in or very close to the conduction band,[6–8] and cannot normally be experimentally observed. The other two p orbitals capture four electrons together. When all six electrons are present in the two shells, as a result of the difference in eigen energies, the thermal emission rate of electrons in the p states will be much higher than for the s electrons. Furthermore for the two s electrons, there is a Coulomb-induced energy difference of a few millielectron volts that was omitted from our previous work.[9] As the normal experimental temperature range for investigations of thermal electron emission from the s shell[12–14] is not lower than about 60 K, this interval is within kT. Therefore, from a statistical point of view, it is reasonable to lump these two energy levels together in the following treatment and consider the s shell to have the same energy level for both the one- and two-electron states. This gives the electron energy scheme shown in Fig. 1. For the thermal emission from the s level of this arrangement, two paths exist: direct emission from the level to the conduction band, or a two-step process across the p level.

In this paper, we present a theory for thermal emission of electrons from QDs, where the dots are treated using a grand canonical ensemble. By specializing in InAs/GaAs dots with base/height dimensions of 20/10 (nm) and taking into account the two possible thermal emission paths, expressions for measurable thermal emission rates are derived. We demonstrate that the thermal emission of electrons from the quantum dot s shell to the host material gradually changes from being dominated by a two-step excitation process via the p shell at the lower temperatures, to a direct emission at the higher temperatures. The transition temperature region is determined by the time it takes for an electron excited to the

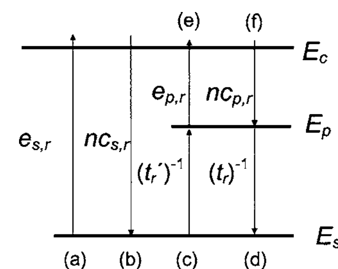

FIG. 1. Energy scheme for an InAs/GaAs quantum dot with base/height dimensions 20/10 nm. For larger dots, a level with d character appears closer to the conduction band at E_c. Arrows (a) and (c)–(e) indicate the two possible thermal emission paths for s electrons while arrows (b) and (d)–(f) show the corresponding capture paths.

    ©2005 The American Physical Society

p energy level to relax back to the s level. The influence of this effect on experimental data is pointed out.

II. QUANTUM DOTS IN THE GRAND CANONICAL ENSEMBLE

Treating QDs with $l=\{1,2,3,\ldots,\}$ eigen state configurations and capable of capturing M electrons, counted by $i=\{1,2,3,\ldots,\}$ in a grand canonical ensemble, the probability $P(r)$ of a QD to capture r electrons is given by

$$P(r)=\frac{\lambda^r Z_r}{\sum_{i=0}^{M}\lambda^i Z_i},\tag{1}$$

where

$$\lambda=\exp\left(\frac{\mu}{kT}\right).\tag{2}$$

Here, μ is the Fermi level, k is Boltzmann's constant, and T is absolute temperature. Z_r is the partition function for a canonical ensemble

$$Z_r=\sum_l \exp\left[-\frac{E(l,r)}{kT}\right],\tag{3}$$

where $E(l,r)$ is the eigen energy for configuration l with r electrons captured.

If the electron states merge into degenerate energy levels, for each r the summation over configurations l can be limited to the configurations available at every specific degenerate level $E(r)$. Furthermore, assuming that the degenerate energy levels are separated by a number of kT units, the summation over l in Eq. (3) can be approximated by a product of the number of permutations g_r of r electrons among the number of available states, and a Boltzmann factor

$$Z_r=g_r\exp\left[-\frac{E(r)}{kT}\right].\tag{4}$$

The ratio $P(r-1)/P(r)$, is then given by Eqs. (1) and (4) as

$$\frac{P(r-1)}{P(r)}=\frac{1}{\lambda}\frac{g_{r-1}}{g_r}\exp\left\{\frac{E(r)-E(r-1)}{kT}\right\}.\tag{5}$$

Taking e_r as the thermal emission rate of electrons, from a QD with r QD electrons captured, to the conduction band, and c_r as the capture rate for an electron in the conduction band to become the r-th captured electron in the QD, we have at thermal equilibrium

$$e_rP(r)=c_rnP(r-1).\tag{6}$$

Here, $n=N_c\exp[-(E_c-\mu)/(kT)]$ is the concentration of electrons in the conduction band, N_c is the effective density of states in the conduction band, and E_c is the energy position of the conduction band edge. Using Eq. (5) in Eq. (6), we get

$$e_r=\frac{g_{r-1}}{g_r}c_rN_c\exp\left\{-\frac{E_c-[E(r)-E(r-1)]}{kT}\right\}.\tag{7}$$

It should be noticed that the difference $E(r)-E(r-1)$ is the energy added to the ensemble when adding one electron. Assuming, for example, that the first i electrons are captured to the same degenerate energy level, all energy differences $E(r)-E(r-1)$ up to $r=i$ have the same value. For InAs/GaAs QDs with base/height dimensions of about 20/10 nm, where two energy levels with s and p characters, respectively, occur,[8] the s shell is two-fold, and the p shell is fourfold degenerate. This means that

$$E(r)-E(r-1)=\begin{cases}E_s, & r=1,2,\\ E_p, & r=3,4,5,6,\end{cases}\tag{8}$$

The thermal emission rate for the s electrons when r electrons are captured in the QDs, therefore, can be expressed as

$$e_{s,r}=\frac{g_{s,r-1}}{g_{s,r}}c_{s,r}N_c\exp\left\{-\frac{\Delta E_s}{kT}\right\},\quad r=1,2,\tag{9}$$

and for the p electrons

$$e_{p,r}=\frac{g_{p,r-1}}{g_{p,r}}c_{p,r}N_c\exp\left\{-\frac{\Delta E_p}{kT}\right\},\quad r=1,2,3,4,\tag{10}$$

where $\Delta E_s=E_c-E_s$ and $\Delta E_p=E_c-E_p$ and E_c is the conduction band edge level. In the following, we assume that $\Delta E_s-\Delta E_p$ is larger than a few kT units. This enables one to treat the two energy levels as independent[2,5] and motivates counting r from 1 to 4 in Eq. (10) instead of using the total number (i.e., $r=3,\ldots,6$).

Due to the different physical properties of the QD crystal and the host, the electron potential, and thus the electron eigen energies, may be influenced by lattice strain and by the energy band-gap off-set values. A certain influence on energy eigen values by temperature is then expected

$$\Delta E_x=\Delta E_x^0-\alpha_xT,\quad x=s,p.\tag{11}$$

If the α_x coefficient is constant, ΔE_x^0 is the energy eigen value at zero temperature. In practice, α_x is often temperature dependent, which means that ΔE_x^0 can be taken as the eigenvalue extrapolated to zero temperature from a linearized temperature region of Eq. (11). Understanding the factor α_x as an entropy contribution from the lattice, the total entropy $\Delta S_{x,r}$ associated with a captured electron can be expressed by

$$\Delta S_{x,r}=\alpha_x+k\ln\frac{g_{x,r-1}}{g_{x,r}}.\tag{12}$$

Introducing a free energy, $\Delta F_{x,r}=\Delta E_x^0-\Delta S_{x,r}T$, the thermal emission rates in Eqs. (9) and (10) can now be expressed in two alternative ways depending on the energy quantity used in the Boltzmann factor

$$e_{x,r}=X_{x,r}c_{x,r}N_c\exp\left\{-\frac{\Delta E_x^0}{kT}\right\}\equiv c_{x,r}N_c\exp\left\{-\frac{\Delta F_{x,r}}{kT}\right\},\tag{13}$$

where

$$X_{x,r}\equiv\exp\left(\frac{\Delta S_{x,r}}{k}\right)\tag{14}$$

is an entropy factor expressing the influence of the total entropy change connected with electron emission and capture.

TABLE I. Possible configurations and associated degeneracy factors for a quantum dot with a maximum of three electrons. The ratios $g_{x,r-1}/g_{x,r}$ are obtained by taking into consideration that the possible permutation number for an empty level is 1, for a single electron on the s level it is 2, for two electrons on the s level it is 1, and for a single electron on the p level it is 4.

Configuration	(a)	(b)	(c)	(d)	(e)
$g_{x,r-1}/g_{x,r}$	$g_{p,0}/g_{p,1}=1/4$	$g_{s,1}/g_{s,2}=2/1$	$g_{s,0}/g_{s,1}=1/2$	$g_{p,0}/g_{p,1}=1/4$	$g_{p,0}/g_{p,1}=1/4$

The first part of Eq. (13) is to be used in the interpretation of activation plots while the second part should be used for data taken at constant temperature, e.g., when the Fermi level is used as a probe to detect an energy level.[10]

The degeneracy factors $g_{x,r-1}/g_{x,r}$ in Eq. (12) are different for different combinations of x and r depending on the carrier configuration from which the emission takes place. Table I demonstrates the possibilities available, assuming that we limit the study to a maximum of three captured electrons.

III. THERMAL EMISSION RATES FOR InAs/GaAs QUANTUM DOTS

In the treatment below, we will take into account the emission of two s electrons and one p electron, which means that cases (a)–(c) of Table I are treated. This limitation is consistent with what normally is found in experiments. As the energy separation between the two levels is normally larger than a few kT, the thermal emissions of electrons from each of the two shells are regarded as independent.[2,5]

After emission of the p electrons, the two s electrons left in the QD may each be emitted through two different channels as depicted in Fig. 1. The first s electron emitted may go directly to the conduction band or via one of the p states, as arrows (a) and (c) indicate in the figure. The second s electron has the same possibilities but based on different magnitudes of the quantum statistical parameters. The electron emission, therefore, consists of an independent thermal process from the p shell [arrow (e) in Fig. 1] and from a coupled two-electron system in the s shell [arrows (a) and (c)–(e) in Fig. 1]. For the analysis of such a system we use the arguments developed for "truncated cascade capture" as discussed in Ref. 11 and slightly altered in Ref. 5. For this treatment, the different emission rates associated with different emission channels are lumped into one *effective* emission rate $e_{e,r}$ as shown for the two electrons in Fig. 2 as discussed below.

The process marked $e_{p,r}$ in Fig. 1 is much faster than the process labeled $e_{s,r}$ due to the difference in binding energy and is given by

$$e_{p,3} = c_{p,3} N_c X_{p,3} \exp\left(-\frac{\Delta E_p^0}{kT}\right). \tag{15}$$

This process is followed by the emission of the s electrons. We consider the energy level system in Fig. 1 and let it represent the situation when emitting an electron thermally from the s states of the quantum dots studied here.

For the transfer between the s and p levels we introduce two time constants: t_r' for the excitation from s to p and t_r for the relaxation from p to s. The portion of the total cycle time, $t_r + t_r'$, spent by the electrons in the p states is given by the ratio $t_r/(t_r + t_r')$. This is the relative time slot open for emission of an electron in the p state to the conduction band. The total emission time $t_{t,r}$ for an electron stepping from s to p and from there to the conduction band is thus given by

$$t_{t,r} = t_r' + \left[\frac{t_r}{t_r + t_r'} e_p\right]^{-1}, \quad r = 1,2. \tag{16}$$

The effective emission rate can now be expressed as the sum of the thermal emission rate $e_{s,r}$ for excitation from the s level to the conduction band and the inverse of $t_{t,r}$

$$e_{e,r} = e_{s,r} + t_{t,r}^{-1}. \tag{17}$$

At thermal equilibrium, we expect

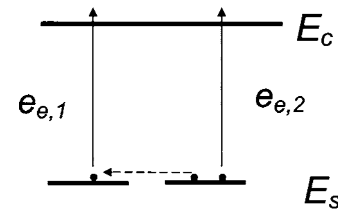

FIG. 2. Energy scheme illustrating the electron "effective emission rates" from a single-level two-electron system. The first electron leaves with a rate $e_{e,2}$ from the s shell, occupied by two electrons, and turns the QD into a one-electron system (dashed arrow). This increases the concentration of one-electron systems before the second electron leaves with a rate $e_{e,1}$.

$$t_r^{-1}P_{p,r} = (t'_r)^{-1}P_{s,r}, \tag{18}$$

where $P_{s,r}$ and $P_{p,r}$ are the probabilities for an electron to occupy the s and p levels, respectively. These two quantities are related by (see Sec. 4.1 in Ref. 5)

$$\frac{P_{s,r}}{P_{p,r}} = \frac{X_{p,r}}{X_{s,r}}\exp\left(\frac{\Delta E_s^0 - \Delta E_p^0}{kT}\right). \tag{19}$$

From Eqs. (18) and (19), assuming that $\Delta E_s^0 - \Delta E_p^0$ is large enough compared to kT, we find $t_r \ll t'_r$ so that Eq. (16) can be approximated as

$$t_{t,r} = t'_r + \frac{t'_r}{t_r}\frac{1}{e_{p,r}}. \tag{20}$$

From Eq. (9) together with Eqs. (17)–(20), we find the effective emission rate

$$e_{e,r} = (c_{s,r} + \Theta_r c_{p,r})X_{s,r}N_c\exp\left(-\frac{\Delta E_s^0}{kT}\right), \tag{21}$$

where

$$\Theta_r = (1 + t_r e_{p,r})^{-1} \tag{22}$$

is a "sticking probability" expressing the tendency for an electron to stay on the p level.[11]

Considering Eq. (21), one observes that the effective thermal emission process from the s shell is made up of two parts. The first part, with the capture rate $c_{s,r}$ for electrons into the s state in the preexponential factor, corresponds to the direct transitions between the s level and the conduction band [arrows (a) and (b) in Fig. 1]. The second part expresses the two-step transitions between the s state and the conduction band via the p state, involving the capture rate to the p level and the sticking probability Θ_r [arrows (c)–(e) and (d)–(f) in Fig. 1].

IV. THERMAL EMISSION OF ELECTRONS FROM A SINGLE-LEVEL TWO-ELECTRON SYSTEM

With the effective emission rates from the s shell defined, we can now treat the system as the single-level two-electron system, shown in Fig. 2. The concentration n_{s2} of QDs which have two electrons in the s shell has a time evolution determined by

$$\frac{dn_{s,2}}{dt} = -e_{e,2}n_{s,2}. \tag{23}$$

Every electron emitted from the two-electron system leaves behind a single-electron system and increases the concentration n_{s1} of QDs occupied by one electron. Taking further into account the emission of the last electron gives the following time evolution of $n_{s,1}$:

$$\frac{dn_{s,1}}{dt} = e_{e,2}n_{s,2} - e_{e,1}n_{s,1}. \tag{24}$$

As boundary conditions we take $n_{s,1}(0)=0$ and $n_{s,2}(0)=N_T$, where N_T is the total concentration of QDs. We find for the time dependence of the electron occupation

$$n_{s,2}(t) = N_T\exp(-e_{e,2}t), \tag{25}$$

$$n_{s,1}(t) = \frac{e_{e,2}}{e_{e,2} - e_{e,1}}N_T[\exp(-e_{e,1}t) - \exp(-e_{e,2}t)]. \tag{26}$$

The concentration p_T of empty dots and dots filled by one and two electrons, respectively, sum up to the total concentration of dots, N_T

$$p_T(t) + n_{s,1}(t) + n_{s,2}(t) = N_T. \tag{27}$$

In deep-level transient spectroscopy (DLTS),[12–14] the transients expressed by Eqs. (25) and (26) are measured as changes of charge in a semiconductor depletion region. During the process of emitting electrons from the dots, each dot occupied by one electron gives rise to a change of one elementary charge and each empty dot gives rise to a change of two elementary charges in the space charge region. The concentration of elementary charges Δp_C produced in the space charge region during the emission process is, by using Eq. (27)

$$\Delta p_C(t) = 2p_T + n_{s,1} + (N_T - n_{p,3}) = 3N_T - n_{s,1}(t) - 2n_{s,2}(t) - n_{p,3}(t), \tag{28}$$

where the time dependencies of $n_{s,1}$ and $n_{s,2}$ are given by Eqs. (25) and (26), respectively, while n_{p3} is determined by the same kinetics as $n_{s,2}$ in Eq. (25)

$$n_{p,3} = N_T\exp(-e_{p,3}t), \tag{29}$$

and where $e_{p,3}$ is given by Eq. (15).

As long as the charge represented by Δp_C is much smaller than the total charge in the space charge region, it is proportional to the amplitude of the capacitance transient obtained from a DLTS measurement.[12–14]

V. ACTIVATION PLOTS AND EMISSION TRANSIENTS

For calculation purposes, we rewrite Eq. (21) in the following way:

$$e_{e,r} = (Y_{s,r} + \Theta_r Y_{p,r})T^2\exp\left(-\frac{\Delta E_s}{kT}\right), \quad r = 1,2 \tag{30}$$

where

$$Y_{s,r} = A\sigma_{s,r}X_{s,r}, \quad r = 1,2, \tag{31}$$

$$Y_{p,r} = A\sigma_{p,r}X_{s,r}, \quad r = 1,2. \tag{32}$$

Here, we have used the relation $c_{s,r}=\langle v\rangle\sigma_{s,r}$, where the average thermal electron velocity $\langle v\rangle$, is set to $\langle v\rangle=(3kT/m^*)^{1/2}$ with m^* representing the electron effective mass in the GaAs conduction band while $\sigma_{s,r}$ and $\sigma_{p,r}$ are the capture cross section for electrons of the s and the p levels, respectively. For the effective density of states in the GaAs conduction band we have used the relation $N_c=4.45\times10^{17}$ $(T/300)^{3/2}$ cm^{-3} which gives $A=3.51\times10^{24}$ $[\text{s}^{-1}\,\text{K}^{-2}]$.

For our calculations of the emission rates we use values for the capture cross section obtained experimentally in an earlier study,[10] where we determined the values for the first

TABLE II. Quantities used in the numerical calculations of Figs. 3 and 4.

$\sigma_{s,1}$ (cm^2)	$\sigma_{s,2}$ (cm^2)	$\sigma_{p,3}$ (cm^2)	$X_{s,1}$	$X_{s,2}$	$X_{s,3}$	ΔE_s (meV)	ΔE_p (meV)
2×10^{-12}	2×10^{-12}	2×10^{-11}	1/2	2	1/4	150	100

captured electron into the QDs. It has been demonstrated in intraband spectroscopy that the capture at low temperature occurs by a two-step process, first into the p shell and from there to the s shell.[15] The values of the capture cross sections measured in Ref. 10, therefore, should be taken as those of the p shell as given in Table II. As the direct transition from the conduction band to the s shell has not been observed in luminescence, it is reasonable to assume that the capture cross sections are smaller for such a process than for the capture into the p shell. In the calculations below, we set capture cross sections for direct transitions to the s shell one order of magnitude smaller than those to the p shell. The internal relaxation time t_r has been investigated in a number of published works on InAs/GaAs QDs. It seems to depend on the physical properties of the dot structures and varies between different works[16–19] in the interval $10^{-12}-10^{-9}$ s. Therefore, the calculations below have been done with t_r varying in this region.

Figure 3 shows the sticking probability Θ_1, given by Eq. (22) as a function of inverse absolute temperature, $1000/T$, for four different values of the internal relaxation time t_1. Θ_2 has a similar shape. At higher temperatures, Θ_1 approaches zero because of the high value of the emission rate $e_{p,1}$. When the temperature is lowered and $e_{p,1}$ decreases, Θ_1 increases within a limited temperature interval depending on the value of t_1 and approaches unit value. This influences the effective thermal emission rates $e_{e,1}$, given by Eq. (21), as shown in Fig. 4. The change in sticking probability separates two different regions of the activation curve for the emission rates. At the higher temperatures the direct emission process from the s shell to the conduction band dominates, while for the lower temperatures, the emission is dominated by the two-step excitation from the s to the p shell and further to the conduction band. The slopes of the two sections in Fig. 4 are the same because the two different emission paths require the same energy as seen from Eq. (23) and illustrated by Fig. 1.

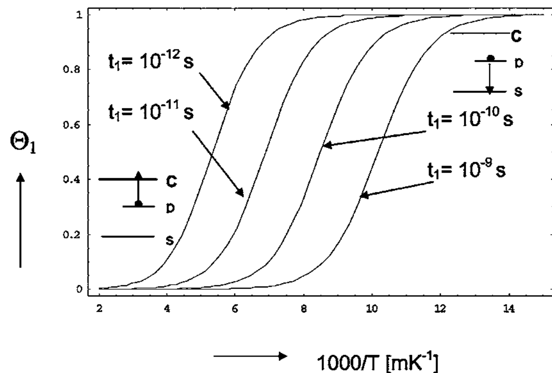

FIG. 3. Sticking probability of the $(s,1)$ electron as a function of reciprocal temperature as obtained by Eq. (22) for different values of the time t_1 it takes for an electron to relax from the p level to the s level when the p level is filled by one electron and the s level is empty.

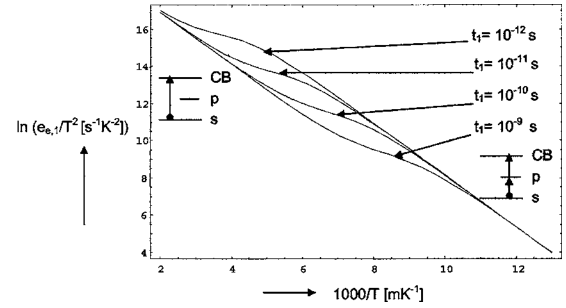

FIG. 4. Thermal emission rate $e_{e,1}$ of an electron from the s level when occupied by one electron as obtained by Eq. (13). For the lower temperatures, the two-step emission path across the p level dominates the emission, while the direct process from the s level to the conduction band dominates for higher temperatures. Between these two temperature regimes, there is a transition region, where the slope of the Arrhenius plot origins from a combination of the two emissions.

The results of the calculation presented in Fig. 4 depend on the values chosen for the entropy factor $X_{s,r}$ which in turn depends on the degeneracy factors and the lattice entropy contribution α_s as expressed by Eq. (12). The degeneracy factors depend on the possible electron configurations as shown in Table I. The actual configurations for $X_{s,1}$ and $X_{s,2}$ to be used in Eq. (21) are those labeled (b) and (c) in Table II, respectively, while the configuration (a) is valid for $X_{p,3}$ to be inserted into Eq. (15). A recent theoretical investigation[20] on the influence of temperature on lattice strain for InAs/GaAs QDs of the present size, indicates that the QD electron potential and the energy eigenvalues are only marginally influenced by a temperature variation between zero and 100 K.

The time dependence of the probabilities for electron occupation, $P_{s1}=n_{s1}(t)/N_T$ and $P_{s2}=n_{s2}(t)/N_T$, respectively, of the s shell during an emission cycle is shown in Fig. 5. The transient P_{s2} falls off exponentially and feeds the increase of P_{s1} before the remaining single-electron occupation decreases as expressed by Eqs. (27) and (28) and illustrated by Fig. 2. The total change of elementary charges in the QDs when emitting one p electron followed by two s electrons, as given by Eq. (30), is shown in the semilogarithmic graph of Fig. 6. The transient is valid for $1000/T=12$, at the low-temperature side of the transition region in Fig. 4 between the two-step and the direct s to conduction band emission. Due to the combination of emission from the p shell and the two electrons in the s shell, the transient has a steep nonexponential shape at the beginning of the time scale for times smaller than about 0.5 μs. For times longer than about 3 μs, a straight line is approached revealing an exponential development. This part reflects the emission of the last electron $(s1)$ leaving the QD. In the intermediate region between 0.5 and 3 μs, the nonexponential behavior originates from a mix

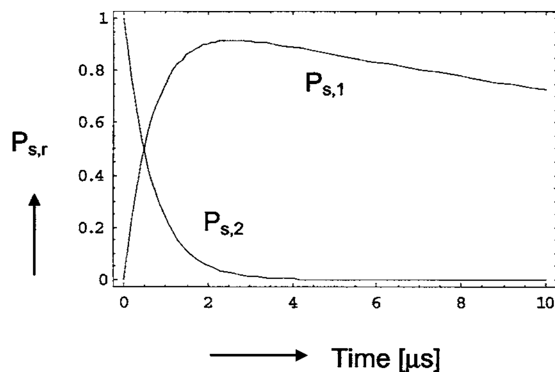

FIG. 5. Emission transients for the first $(s,2)$ and second $(s,1)$ electrons leaving the quantum dot. The curves show the probabilities $P_{s,1}=n_{s,1}/N_T$ and $P_{s,2}=n_{s,2}/N_T$ that the s shell is occupied by one and two electrons, respectively. Calculation has been done for $t_1=t_2=10^{-10}$ s and $1000/T=12$ mK^{-1}

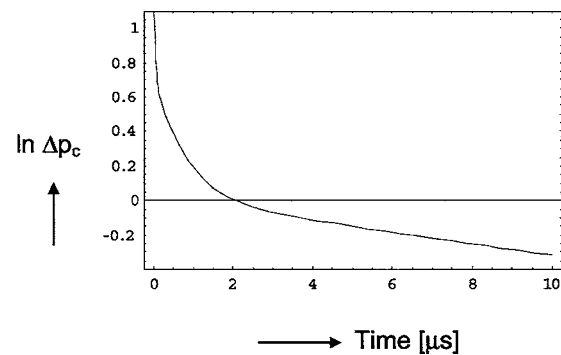

FIG. 6. Logarithm of the charge Δp_c in units of elementary charge, created per quantum dot in a semiconductor depletion region as it would appear in a DLTS measurement for $t_1=t_2=10^{-10}$ s and $1000/T=12$ mK^{-1} as in Fig. 5

of emissions by the two s electrons. These kinds of transients, composed of multielectron emission are expected to be reflected in spectra obtained from deep-level transient data. The two-electron character of the s level and the emission from the p level have been observed in such experimental spectra.[13,14]

VI. DISCUSSION AND CONCLUSIONS

The temperature dependence of the sticking probability, shown in Fig. 3 is strongly influenced by the internal relaxation time t_r' of electrons from the p shell to the s shell indicated by an arrow (d) in Fig. 1. It is related to the so called "phonon bottleneck,"[16–19] often mentioned in the literature, and depends on the availability of phonon energies fitting to the energy difference between the different energy levels in the QD. The relaxation time, therefore, may be expected to be dependent on the sizes, shapes, and chemical compositions of dots. This has a consequence for the interpretation of activations plots for the thermal emission rates of charge carriers. The calculated set of curves in Fig. 4, demonstrates how the relaxation time influences the transition from s to p shell to conduction band at lower temperatures to approach direct emission from the s shell to the conduction band for the higher temperatures. Experimental setups for DLTS, normally used for measuring emission rates, have response times which for the present system limit the measurements to the temperature region below about 100 K. Therefore, the slope of an activation curve may be influenced by the change due to the change of emission path. For the largest values of the relaxation time, there is an obvious risk to misinterpret the values of activation energies and capture rates. In order to avoid such erroneous interpretations, additional and independent measurements of, for example, the capture cross sections may be necessary. For the data used in the present analysis, this was done in earlier work which supported an assumption that the relaxation time was short enough for the transition region to be outside the measured activation plot.[10,13,20]

In DLTS, capacitance transients transformed into temperature spectra are used to find the thermal activation energies related to charge carrier emission. When emissions take place by more than one electron with close lying activation curves, the spectral peaks may interfere and give rise to misleading conclusions. The emission of the two s electrons in the present system has been investigated experimentally in the low temperature range where two-step processes across the p shell take place[13] and the peaks occurring in DLTS spectra could be explained by the spread in QD size.

Thermal emission rates are often measured by DLTS, where the emission sources are placed in a space charge region of a p-n junction or a Schottky diode. Especially for QDs, with the electron eigen energies relatively shallow, in the region of 200 mV and lower, a nonvanishing tunneling rate may add to the thermal emission rate studied for higher applied voltages. This is clearly the case for some of the data in Refs. 12–14 and has a significance for higher voltages and lower temperatures. Tunneling was not included in the present description. Taking into account the tunneling paths from both the s and the p shells, these processes can be added to the thermal processes expressed in Eq. (21) in order to obtain the full expression for electron emission. In this context it should be observed that when a realistic potential for the QD electrons is taken into account[9] the tunneling rates deviate by at least one order of magnitude from those given in the classical paper by Korol,[21] often used in the literature. In this latter case, the calculation was done for deep impurities represented by a delta function and can hardly be used for QDs as demonstrated in Ref. 9.

Grundmann and Bimberg had earlier developed statistics for the capture of electrons into quantum dots.[22] It should be noted that their treatment is valid under nonequilibrium situations and for a high concentration of excess charge carriers in the semiconductor energy bands, i.e., for example, for luminescence experiments. In the present work, we have given the statistics for an experiment where electrons are thermally emitted from quantum dots in a semiconductor depletion region. This is the common situation when measuring thermal emission rates by DLTS. The two treatments, therefore, describe charge-carrier traffic at quantum dots for two different and complementary experimental cases.

*Corresponding author. Email address: olof.engstrom@mc2.chalmers.se

[1] W. Shockley and W. T. Read, Phys. Rev. **87**, 835 (1952).
[2] P. T. Landsberg, *Recombination in Semiconductors* (Cambridge University Press, Cambridge, 1992).
[3] M. J. Kirton and M. J. Uren, Adv. Phys. **38**, 367 (1989).
[4] O. Engström and A. Alm, J. Appl. Phys. **54**, 5240 (1983).
[5] P. T. Landsberg and O. Engström, in *Handbook of Semiconductors*, Vol. 1, edited by P. T. Landsberg (Elsevier, New York, 1992), p. 197.
[6] M. Grundmann, O. Stier, and D. Bimberg, Phys. Rev. B **52**, 11969 (1995).
[7] L.-W. Wang, J. Kim, and A. Zunger, Phys. Rev. B **59**, 5678 (1999).
[8] P. Hawrylak and A. Wojs, Semicond. Sci. Technol. **11**, 1516 (1996).
[9] Y. Fu, O. Engström, and Y. Lou, J. Appl. Phys. **96**, 6477 (2004); Y. Fu, Y. Lou, and O. Engström (unpublished).
[10] O. Engström, M. Kaniewska, Y. Fu, J. Piscator, and M. Malmkvist, Appl. Phys. Lett. **85**, 2908 (2004).
[11] P. T. Landsberg and S. R. Dhariwal, Phys. Rev. B **39**, 91 (1989).
[12] C. M. A. Kapteyn, F. Heinrichsdorff, O. Stier, R. Heitz, M. Grundmann, N. D. Zakharov, and D. Bimberg, Phys. Rev. B **60**, 14265 (1999).
[13] O. Engström, M. Malmkvist, Y. Fu, H. Ö. Olafsson, and E. Ö. Sveinbjörnsson, Appl. Phys. Lett. **83**, 3578 (2003).
[14] S. Schulz, S. Schnull, Ch. Heyn, and W. Hansen, Phys. Rev. B **69**, 195317 (2004).
[15] T. Müller, F. F. Schrey, G. Strasser, and K. Unterrainer, Appl. Phys. Lett. **83**, 3572 (2003).
[16] F. Adler, M. Geiger, A. Bauknecht, F. Scholz, H. Schweizer, and M. H. Pilkuhn, J. Appl. Phys. **80**, 4019 (1996).
[17] S. Malik, E. C. Le Ru, D. Childs, and R. Murray, Phys. Rev. B **63**, 155313 (2001).
[18] R. Heitz, H. Born, F. Guffarth, O. Stier, A. Schliwa, A. Hoffmann, and D. Bimberg, Phys. Rev. B **64**, 241305(R) (2001).
[19] E. Tsitsishvili, R. v. Baltz, and H. Kalt, Phys. Rev. B **66**, 161405(R) (2002).
[20] O. Engström, Y. Fu, and A. Eghtedari, Physica E (Amsterdam) **27**, 380 (2005).
[21] E. N. Korol, Sov. Phys. Solid State, **19**, 1327 (1977).
[22] M. Grundmann and D. Bimberg, Phys. Rev. B **55**, 9740 (1997).